Direct evidence for mode-specific vibrational energy relaxation from quantum time-dependent perturbation theory. I. Five-coordinate ferrous iron porphyrin model

Yong Zhang,[a] Hiroshi Fujisaki,[b] and John E. Straub[c]
Department of Chemistry, Boston University, Boston, Massachusetts 02215, USA

(Received 16 October 2008; accepted 3 December 2008; published online 13 January 2009)

The time scales and mechanisms of mode-specific vibrational energy relaxation in imidazole ligated ferrous iron porphine were studied using a non-Markovian time-dependent perturbation theory and density functional theory calculation. Seven normal modes, including ν_4, ν_7, and five Fe out-of-plane modes (Fe-oop), were treated as the relaxing system mode coupled to all other modes forming the bath. The derived cooling time constants for the ν_4 and ν_7 modes agree well with the results of previous experimental studies. The pathways for energy transfer from each system mode were identified. The γ_7 mode, associated with Fe-oop motion with frequency ~ 350 cm^{-1}, was observed to couple strongly through its overtone with the ν_7 porphine in-plane vibration. This suggests a possible mechanism for the excitation of the ν_7 mode, which is distinct from the direct excitation together with Fe-oop motion of the ν_4 mode. Four other Fe-oop motions were observed to couple to low frequency modes including those involving significant imidazole ligand motions. Through these couplings, excitation following ligand photodissociation may be efficiently transferred from the heme doming mode to the protein backbone motions essential to conformational changes associated with the protein's function. © *2009 American Institute of Physics*. [DOI: 10.1063/1.3055277]

I. INTRODUCTION

In myoglobin (Mb) or hemoglobin (Hb), ligand dissociation can occur when the ligand-heme complex absorbs a visible or UV photon. Photoexcitation can cause vibrational excitation of the ligand, heme, and the surrounding residues.[1,2] Understanding the time scales and mechanisms of vibrational energy excitation and relaxation that follow such events is an essential component of an understanding of the ultrafast conformational changes associated with protein function. Much experimental and theoretical work has explored this subject.[3–25]

Using time-resolved resonance Raman spectroscopy, Mizutani and co-workers[26–29] monitored the intriguing mode-specific behavior of heme vibrational relaxation following ligand dissociation. It was found that the ν_4 and ν_7 modes were highly excited during the reaction, and the decay time constants were found to be 1.1 ± 0.6 ps for the ν_4 band and 1.9 ± 0.6 ps for the ν_7 band, implying a thermal decay of the heme within 2 ps.[28,29] As a model of the heme moiety, metalloporphyrins have been studied,[30–32] and the mode-specific properties observed.[33–35] For nickel octaethylporphyrin (NiOEP) in organic solvents, the relaxation of both the ν_4 and the ν_7 modes was found to have a fast phase with time constants ~ 10 ps and a slow phase with time constants longer than 300 ps. For iron(III) *meso*-tetrakis(4-sulfonatopheyl)porphyrin (FeTPP), the fast phase was found to be 1.9 ± 0.4 ps, whereas the slow phase depends on the ratio of the solvent components.[34]

The low frequency heme modes (<400 cm^{-1}) were studied using femtosecond coherence spectroscopy in Refs. 36–41. Using a 50 fs pulse, a series of modes at ~ 40, ~ 80, ~ 130, and ~ 170 cm^{-1} were observed for several myoglobin derivatives.[42] The couplings between these modes were suggested. Using a sub-10-fs pulse, Miller and co-workers[18,43] extended the range of the coherence spectroscopy to higher frequencies (up to 3000 cm^{-1}). The heme ν_7 mode was found to be most strongly excited following Q band excitation. By comparing to the deoxyMb spectrum, they demonstrated that the signal was "reaction driven," derived from the structural transition from the six-coordinate to the five-coordinate heme. Less prominent excitation of the ν_4 mode was also observed. The selective excitation of the ν_7 mode, following excitation of out-of-plane heme doming, led to the intriguing conjecture that there may be directed energy transfer of the heme excitation to motions connected to backbone displacement and to protein function.

Anfinrud and co-workers[44] studied heme cooling in myoglobin and observed single-exponential decay kinetics with a time constant of 6.2 ± 0.5 ps. Using molecular dynamics simulation, Sagnella and Straub[45] and Bu and Straub[46] found that the decay of the heme excess kinetic energy following ligand dissociation is a single-exponential process with a time constant of 5.9 ps for both wild type sperm whale myoglobin and the H93G mutant. The strong interaction between the isopropionate side chains and the solvent water molecules was conjectured to be the dominant

[a]Electronic mail: zhangy@bu.edu.
[b]Present address: Integrated Simulation of Living Matter Group, Computational Science Research Program, RIKEN, Japan.
[c]Author to whom correspondence should be addressed. Electronic mail: straub@bu.edu.

pathway for excess energy dissipation from the heme. This conjecture was supported by subsequent experimental studies.[47–49]

In spite of years of intensive and inventive study, the detailed process of energy transfer following ligand dissociation is still not fully understood, and many open questions remain. How are the ν_4 and ν_7 modes excited, and how is the excess energy dissipated? What is the role of the covalent bond between Fe and His93 in the heme cooling process? By comparing the crystal structures, it was found that carbonmonoxymyoglobin and deoxymyoglobin have distinct tertiary structures.[50] How is ligand dissociation and subsequent heme cooling connected to this global protein structural change?

To address these questions, we carried out quantum chemical density functional theory (DFT) studies of a five-coordinate heme model, imidazole (Im) ligated ferrous iron porphine (FeP-Im). Using a time-dependent perturbation theory,[51] for the dynamics of a single "system mode" coupled to surrounding "bath modes," the mode-specific vibrational energy transfer process was examined. The ν_4 mode, ν_7 mode, and five modes involving Fe out-of-plane motion (Fe-oop) were independently treated as the system mode, and the vibrational energy relaxation (VER) time scale and pathways were identified. The resulting VER time constants of the ν_4 and ν_7 modes agree well with previous experimental results. Strong coupling between the γ_7 Fe-oop motion and in-plane ν_7 mode is predicted providing a possible explanation for the preferential excitation of the ν_7 mode following ligand photolysis in MbCO observed by Miller and co-workers. The coupling between Fe-oop modes with low frequency motions is identified and its relation to global protein structural relaxation discussed.

II. THEORY AND METHODS

A. Non-Markovian time-dependent perturbation theory

The VER rate formula employed in this work[51,52] is briefly summarized. We expand the potential energy surface with respect to the normal coordinates of the system, q_S, and bath, q_α, and their frequencies up to third and fourth order nonlinear couplings

$$H = H_S + H_B - q_S \delta F + q_S^2 \delta G, \tag{1}$$

$$H_S = \frac{p_S^2}{2} + V(q_S), \tag{2}$$

$$H_B = \sum \left(\frac{p_\alpha^2}{2} + \frac{\omega_\alpha^2 q_\alpha^2}{2} \right), \tag{3}$$

$$\delta F = \sum_{\alpha,\beta} C_{S\alpha\beta}(q_\alpha q_\beta - \langle q_\alpha q_\beta \rangle), \tag{4}$$

$$\delta G = \sum_{\alpha,\beta} C_{SS\alpha\beta}(q_\alpha q_\beta - \langle q_\alpha q_\beta \rangle) + \sum_\alpha C_{SS\alpha} q_\alpha, \tag{5}$$

where H_S (H_B) is the system (bath) Hamiltonian and $C_{S\alpha\beta}$ ($C_{SS\alpha\beta}$) are the third (fourth) order coupling terms. From the von Neumann–Liouville equation, a reduced density matrix for the system mode is derived using the time-dependent perturbation theory after tracing over the bath degrees of freedom. The commonly employed Markov approximation is avoided, and no assumption of a separation in time scales between system and bath mode relaxation is invoked in this theory. The final VER formula is obtained,

$$\begin{aligned}(\rho_S)_{00}(t) \simeq \frac{2}{\hbar^2}\sum_{\alpha,\beta} [&C_{--}^{\alpha\beta} u_t(\tilde{\omega}_S - \omega_\alpha - \omega_\beta) \\ &+ C_{++}^{\alpha\beta} u_t(\tilde{\omega}_S + \omega_\alpha + \omega_\beta) + C_{+-}^{\alpha\beta} u_t(\tilde{\omega}_S - \omega_\alpha + \omega_\beta)] \\ &+ \frac{2}{\hbar^2}\sum_\alpha [C_-^\alpha u_t(\tilde{\omega}_S - \omega_\alpha) + C_+^\alpha u_t(\tilde{\omega}_S + \omega_\alpha)],\end{aligned} \tag{6}$$

where the subscript of $(\rho_S)_{00}$ indicates the vibrational ground state and $u_t(\Omega)$ is defined as

$$u_t(\Omega) = \int_0^t dt' \int_0^{t'} dt'' \cos \Omega(t' - t'') = \frac{1 - \cos \Omega t}{\Omega^2}. \tag{7}$$

The coefficients, $C_{--}^{\alpha\beta}$, $C_{++}^{\alpha\beta}$, $C_{+-}^{\alpha\beta}$, C_-^α, and C_+^α, can be derived from the nonlinear coupling constants $C_{S\alpha\beta}$ and $C_{SS\alpha\beta}$ as

$$\mathbf{C}^{\alpha\beta} = \begin{pmatrix} C_{--}^{\alpha\beta} & C_{+-}^{\alpha\beta} \\ C_{+-}^{\alpha\beta} & C_{++}^{\alpha\beta} \end{pmatrix} = \{(q_S)_{10} C_{S\alpha\beta} - (q_S^2)_{10} C_{SS\alpha\beta}\}^2 \mathbf{S}^{\alpha\beta}, \tag{8}$$

$$\mathbf{S}^{\alpha\beta} = \frac{\hbar^2}{2\omega_\alpha\omega_\beta} \begin{pmatrix} (1+n_\alpha)(1+n_\beta) & 2(1+n_\alpha)n_\beta \\ 2(1+n_\alpha)n_\beta & n_\alpha n_\beta \end{pmatrix}, \tag{9}$$

$$\mathbf{C}^\alpha = \begin{pmatrix} C_-^\alpha \\ C_+^\alpha \end{pmatrix} = (q_S^2)_{10}^2 C_{SS\alpha}^2 \mathbf{R}^\alpha, \tag{10}$$

$$\mathbf{R}^\alpha = \frac{\hbar}{2\omega_\alpha} \begin{pmatrix} 1+n_\alpha \\ n_\alpha \end{pmatrix}, \tag{11}$$

where $n_\alpha = 1/(e^{\beta\hbar\omega_\alpha} - 1)$ is the thermal phonon number. When the system mode is excited to the $\nu = 1$ state, VER is described by the decay of the reduced density matrix element $\rho_{11}(t) = 1 - \rho_{00}(t) \simeq \exp[-\rho_{00}(t)]$ with only the normal mode frequencies of the model system and the nonlinear coupling constants $C_{S\alpha\beta}$ and $C_{SS\alpha\beta}$ as input.

B. Simulation and analysis protocol

As a model of the heme following ligand photodissociation in Mb, the five-coordinate imidazole ligated ferrous iron porphine (FeP-Im) was studied. The structure was optimized to its ground state, the quintuplet state,[53–56] at the UB3LYP/6-31G(d) level. The "very tight" self-consistent field (SCF) convergence criterion and "ultrafine" integration grid were applied in the calculation. The normal mode analysis was carried out for the optimized structure. The third and fourth order anharmonic coupling constants were calculated using a finite difference method.[57] All calculations was carried out using the GAUSSIAN03 package.[58]

The system mode vibrational energy transfer rate constant was derived by fitting the reduced density matrix element $\rho_{11}(t)$ time profile to a single exponential decay func-

TABLE I. The calculated and experimentally measured relative energies and selected geometrical parameters for different spin states of FeP-Im.

	E_{rel} (kcal/mol)	d_{Fe-P} (Å)	d_{Fe-N} (Å)	$d_{Fe-N(Im)}$ (Å)
Singlet	7.0	0.153	2.001	1.924
Triplet	13.2	0.108	2.001	2.249
Quintuplet	0.0	0.311	2.085	2.164
Expt. (quintuplet)[a]	···	0.42	2.086	2.161
Expt. (deoxyMb)[b]	···	0.290	2.057	2.15

[a]Data for Fe(II)TPP(2Me-Im) (Ref. 66).
[b]Data for deoxyMb (Ref. 50).

tion. The energy transfer pathways were identified by calculating the third order Fermi resonance parameters defined as[59,60]

$$r_{S\alpha\beta} = \frac{|C_{S\alpha\beta}|}{\hbar|\tilde{\omega}_S - \omega_\alpha - \omega_\beta|}\sqrt{\frac{\hbar}{2\tilde{\omega}_S}}\sqrt{\frac{\hbar}{2\omega_\alpha}}\sqrt{\frac{\hbar}{2\omega_\beta}}, \tag{12}$$

where $\tilde{\omega}_S$ and ω_α are the frequencies of the system mode and bath modes, respectively.

It has been observed that vibrational modes involved in the most effective energy transfer pathways have large overlap in space with the system mode. As a quantitive measure, the geometrical overlap of the system mode, S, and bath modes, α and β, was calculated following the definition of Kidera and co-workers,[61]

$$G_3(S,\alpha,\beta) = \sum_{i=1}^{N_{atom}} m_i^{3/2}|\mathbf{v}_{iS}||\mathbf{v}_{i\alpha}||\mathbf{v}_{i\beta}|, \tag{13}$$

where N_{atom} is the number of atoms in the molecule, m_i is the mass of atom i, and $\mathbf{v}_{i\alpha}$ is the calculated eigenvector for mode α and atom i. Large values of G_3 imply strong spatial overlap of the system and designated bath modes.

III. RESULTS

A. Calculated structure and frequencies of FeP-Im system

It has been reported that the ground state of imidazole ligated ferrous iron porphyrin is a electronic quintuplet state.[53–56] While previously reported DFT calculations have failed to produce the correct ground state,[62–65] it was successfully predicted in our calculation. The relative energies of FeP-Im at its singlet, triplet, and quintuplet states are summarized in Table I alongside the porphine Fe-oop displacement d_{Fe-P}, core size d_{Fe-N} and Fe-N(Im) distance $d_{Fe-N(Im)}$, both computed and derived from experiments.[50,66]

The optimized porphine structure is nearly planar, as shown in Fig. 1. The displacement of each atom relative to the porphine plane (with the Fe atom at the origin) is shown in Fig. 2, compared to those derived from deoxyMb and MbCO crystal structures [protein data bank (PDB) entries 1BZP (Ref. 50) and 1MBC (Ref. 67), respectively]. The porphine plane is slightly displaced from C_4 symmetry due to the ligation of the imidazole. The porphine is domed with the Fe atom displaced ~0.3 Å from the average plane defined by the four pyrrole N atoms, close to the displacement observed

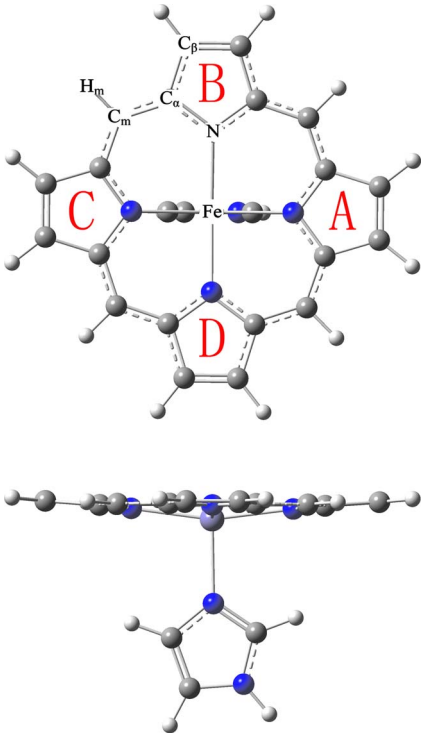

FIG. 1. (Color online) Depiction of the optimized structure of FeP-Im (S =2) at the UB3LYP/6-31G(d) level (top view and side view). The four pyrrole rings, A, B, C, and D, are labeled.

in deoxyMb (see Table I).[50,68] The core size, defined as the distance between the Fe and pyrrole N atoms, was found to be 2.085 Å, which agrees with the distance observed for Fe(II)TPP(2Me-Im) (Ref. 66) and somewhat larger than observed in myoglobin.[50]

The calculated harmonic frequencies are summarized in Table II (only those mentioned in the text or involved in the important VER pathways, a complete list is available in the supplemental material).[69] The contribution to the norm from the porphine ring and from the porphine ring in-plane motion

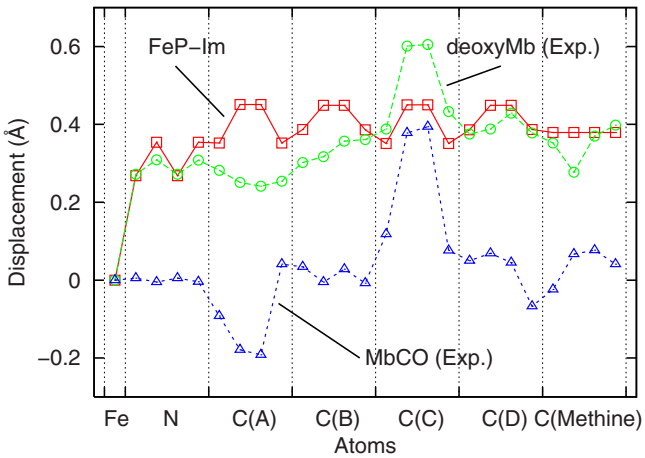

FIG. 2. (Color online) The calculated displacements of the porphine heavy atoms of FeP-Im relative to the porphine plane defined by the four nitrogen atoms (with origin centered at the Fe atom) ordered as the iron, pyrrole nitrogens, pyrrole carbons (A, B, C, and D as shown in Fig. 1), and methine carbons. The displacements derived from deoxyMb and MbCO crystal structures [PDB entries 1BZP (Ref. 50) and 1MBC (Ref. 67)] are provided for reference.

TABLE II. The calculated normal mode frequencies and the contribution to the norm from (1) the porphine ring (vs the imidazole) and (2) from the porphine ring in-plane (vs out-of-plane) motion for each mode of the FeP-Im in its electronic ground state (only those involved in the important VER pathways or mentioned in the text).

Mode number	Frequency (cm^{-1})	Norm of porphyrin	Norm of porphyrin in-plane motion
1	23.3724	0.336	0.080
2	29.5028	0.059	0.021
3	33.3330	0.406	0.088
4	58.0715	0.988	0.007
5	64.5136	0.731	0.003
7	117.9128	0.388	0.027
8	130.0445	0.307	0.039
9	147.8020	0.697	0.026
10	153.3291	0.756	0.015
11	163.0287	0.603	0.021
12	195.6650	0.938	0.645
14	209.6426	0.984	0.071
15	212.6182	0.978	0.025
17	237.1221	0.967	0.925
18	242.1653	0.949	0.028
23	348.5159	1.000	0.191
24	363.3370	1.000	0.804
31	480.6535	1.000	0.005
33	646.7218	0.001	0.000
34	674.3655	1.000	0.009
35	678.5292	1.000	0.006
36	679.6977	0.067	0.001
37	680.9503	0.938	0.009
38	691.7220	0.999	0.006
39	703.1181	1.000	0.004
40	706.9701	0.995	0.008
41	710.2070	1.000	0.006
43	731.5817	0.001	0.000
44	733.0905	1.000	0.992
55	826.0840	0.002	0.002
65	907.2398	1.000	0.005
69	1006.8913	0.999	0.994
82	1160.1371	0.001	0.001
95	1380.7058	0.778	0.775

is given for each mode. The contribution of 1.0 (0.0) from the porphine ring means that the mode is localized in the porphine (imidazole ligand). Similarly, a contribution of 1.0 from the porphine ring in-plane motion indicates a pure porphine in-plane mode.

B. Vibrational energy relaxation in ν_4 mode and ν_7 mode

The frequencies calculated for the ν_4 and ν_7 modes, both in-plane breathing-like motions as demonstrated in Fig. 3, are summarized in Table III. Applying the time-dependent perturbation method described above, the vibrational energy transfer time constant from the excited ν_4 mode was found to be 1.7 ± 0.2 ps. The ν_7 mode was observed to have a longer energy transfer time constant of 2.9 ps (see Table III). The calculated results agree well with the experimentally determined values for heme in MbCO following photodissociation (1.1 ± 0.6 ps for ν_4 mode and 1.9 ± 0.6 ps for ν_7 mode),[27] considering the use of a model system and approximations inherent to the theory. The time evolution of the initially excited density matrix element is shown for each mode in Fig. 4. The inset shows the corresponding time evolution of the important VER pathways.

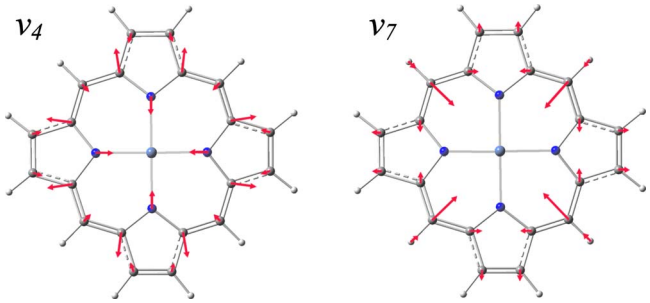

FIG. 3. (Color online) Depiction of the computed porphine ν_4 and ν_7 modes. The ligand imidazole has the same orientation as in Fig. 1 (not shown here).

The energy accepting "doorway" modes define the energy transfer pathways from the excited mode. Those modes were identified by calculating the third order Fermi resonance parameters using Eq. (12). (The higher order parameters were found to be much smaller and were neglected in the analysis.) For each system mode, the calculated third order Fermi resonance parameters $r_{S\alpha\beta}$ of the important VER pathways (defined as $r_{S\alpha\beta} \geq 0.05$) are shown in Fig. 5 as well as the important coupling constants $C_{S\alpha\beta}$ and the frequency resonance parameters $1/|\tilde{\omega}_S - \omega_\alpha - \omega_\beta|$.

For the excited ν_4 mode, most bath modes involved in the important energy transfer pathways are associated with porphine out-of-plane motions (not to be confused with Fe-oop motions). Most of these modes have frequencies near 700 cm^{-1}. Modes 33, 36, 43, 55, and 82 have significant contribution from the ligand imidazole motions. Modes 24 and 69 are associated with pure porphine in-plane motions, and 69+24 forms the only important in-plane mode pathway for relaxation of the ν_4 system mode. No mixed in-plane/out-of-plane combination was found to be important in the energy transfer pathways. No direct energy transfer from the ν_4 to ν_7 mode was observed.

Energy transfer from the excited ν_7 mode was found to have fewer important relaxation pathways. Save mode 24, all modes involved in the relaxation pathway of the ν_7 system mode are porphine out-of-plane motions including mode 23 (assigned as the γ_7 mode), which is associated with Fe-oop motion (see Fig. 6). The excited ν_7 mode is strongly coupled with the overtone of mode 23 through a large third order coupling constant. This coupling will be discussed in detail below.

Following the definition in Eq. (13), the geometrical overlap of each system mode (ν_4 or ν_7) with bath mode combinations was calculated. The results are summarized in the supplemental materials.[69] It was found that all important energy transfer pathways have large geometrical overlap with the system mode. This indicates the importance of geometrical overlap in effective energy transfer pathways as suggested previously by Kidera and co-workers.[61]

TABLE III. Summary of system mode frequencies (harmonic and corrected anharmonic), the VER time constants, and the assignments studied for FeP-Im in its electronic ground state.

	Frequency (cm^{-1})		T_1 (ps)		
Mode number	Harmonic	Anharmonic	Simulation	Experiment[a]	Assignment
95	1380.7	1372.6	1.7 ± 0.2	1.1 ± 0.6	ν_4
44	733.1	729.9	2.9 ± 0.0	1.9 ± 0.6	ν_7
23	348.5	349.2	7.9 ± 0.7		γ_7
18	242.2	238.2	2.5 ± 0.1		γ_{242}
16	230.7	233.5	4.9 ± 0.2		γ_{230}
11	163.0	170.2	7.9 ± 0.9		ν(Fe-Im)
5	64.5	75.8	66.5 ± 81.1		Doming

[a]Data for carboxyMb (Ref. 27).

C. Vibrational energy relaxation in Fe out-of-plane modes

Five modes associated with Fe-oop motion, including mode 23 implicated in the ν_7 relaxation pathway, were identified in the calculation. Three high frequency modes, 23, 18, and 16, do not involve imidazole ligand motion, whereas the two low frequency modes, 11 and 5, are coupled with Im motion. Mode 23 is the porphine methine wagging associated with Fe-oop motion, assigned as γ_7. Modes 18 and 16, at 242.2 and 230.7 cm^{-1}, respectively, are similar in motion (split by the imidazole ligation) and are labeled γ_{242} and γ_{230}, respectively. Mode 11 is assigned as Fe-Im stretching, ν(Fe-Im), and mode 5 as porphine doming. The frequencies of these modes are summarized in Table III and depicted in Fig. 6 with the porphine atom relative displacements indicated by the normalized eigenvectors (scaled by 100). The decay of the time evolution of the density matrix element for each excited Fe-oop mode is fitted by a single exponential function, and the time constants are summarized in Table III. The calculated third order Fermi resonance parameter $r_{S\alpha\beta}$ of the important VER pathways, the coupling constants $C_{S\alpha\beta}$, and the frequency resonance parameter $1/|\tilde{\omega}_S - \omega_\alpha - \omega_\beta|$ are shown in Fig. 7 for each system mode.

Relative to the coupling between the ν_4 and ν_7 system modes and their bath modes, the couplings between Fe-oop motion and their bath modes are relatively weak and associated with smaller Fermi resonance parameters (with exceptions due to close frequency resonance). With the exception of mode 17 for system mode γ_{242}, no pure porphine in-plane mode was involved in the important energy transfer pathways. On the other hand, the imidazole ligand motion appears to be involved in the energy transfer pathways for all excited Fe-oop modes. Specifically, all important energy transfer pathways from the excited ν(Fe-Im) mode involve significant imidazole motions. No strong coupling between the Fe-oop modes was observed. For these bath mode combinations, large geometrical overlap with the system mode was observed.

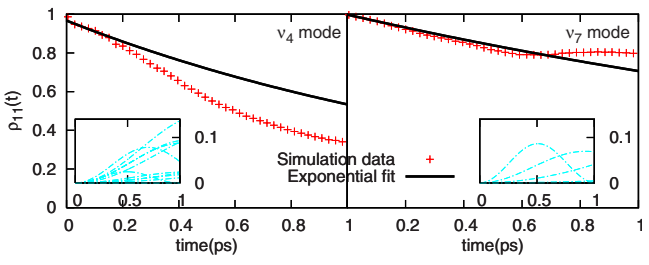

FIG. 4. (Color online) The time evolution of the initially excited density matrix element ρ_{11} for the ν_4 and ν_7 modes. The simulation data are shown as points, and the single-exponential fit to the initial decay is shown as a solid line. The time evolution of ρ_{00} of the important VER pathways is shown in the inset. The fitted time constants are summarized in Table III. For each mode, the calculated third order Fermi resonance parameters of the important VER pathways are plotted in Fig. 5 together with the important coupling constants and the frequency resonance parameters.

IV. DISCUSSION AND ANALYSIS

In MbCO, the Fe-oop motions have received considerable attention due to their role in conformational transitions associated with protein function.[5,43,70–73] It has been suggested that Fe-oop motion is the first event to follow ligand dissociation in Mb or Hb.[74] This local structural change in the heme has long been identified as the motion triggering global conformational change in Mb or Hb essential to intramolecular signaling associated with protein function.[50,68,75–77] In this study of model imidazole ligated ferrous iron porphine, five Fe-oop modes have been identified. The relaxation of these modes, as well as the in-plane ν_4 and ν_7 modes, from vibrationally excited states was studied to gain insight into the time scale and pathways of vibrational population relaxation.

A. Identification of Fe out-of-plane modes

In this work, mode 5 with frequency 64.5 cm^{-1} was identified as the heme doming motion. This is consistent with the general belief that the heme doming motion has a frequency below 100 cm^{-1}.[39,78,79] The Fe-Im stretch, another well studied mode, was identified as mode 11, having frequency 163.0 cm^{-1}. The other three Fe-oop modes, γ_7, γ_{242}, and γ_{230}, do not appear to have been widely studied. In a femtosecond coherence spectroscopy study on 2-methyl imidazole ligated iron-protoporphyrin IX (2MeIm-FePPIX) by Champion and co-workers,[40] a series of signals were observed at 38, 72, 127, 213, 259, and 349 cm^{-1}, respectively. Similar modes were observed in other porphyrin species. Due to the different porphyrin model used in this study, we cannot conclude that these experimentally observed signals

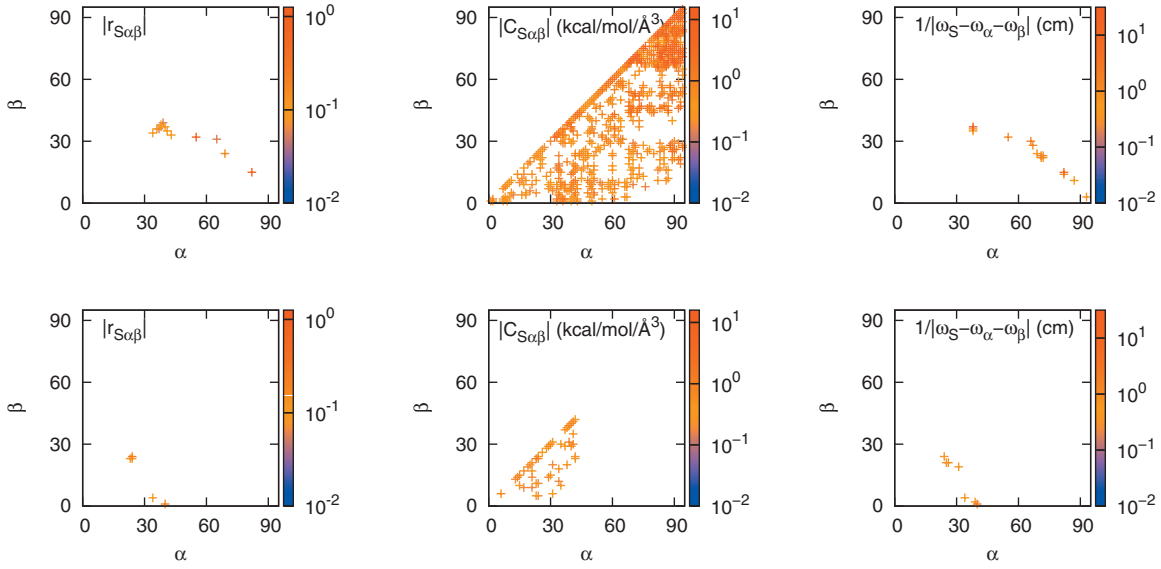

FIG. 5. (Color) The calculated third order Fermi resonance parameters $r_{S\alpha\beta}$ of the important VER pathways for the ν_4 (top) and ν_7 (bottom) modes as well as the important coupling constants $C_{S\alpha\beta}$ and the frequency resonance $1/|\tilde{\omega}_S-\omega_\alpha-\omega_\beta|$. The x and y axes are the indices of the bath modes.

correspond to the modes found in our simulation, having frequencies of 33.3 cm^{-1} (mode 3), 64.5 cm^{-1} (doming), 117.9 cm^{-1} (mode 7), 163.0 cm^{-1} (ν(Fe-Im)), 242.2 cm^{-1} (γ_{242}), and 348.5 cm^{-1} (γ_7), respectively. However, it is reasonable to believe that similar modes exist in the experiments and are involved in the dynamics following heme photoexcitation.

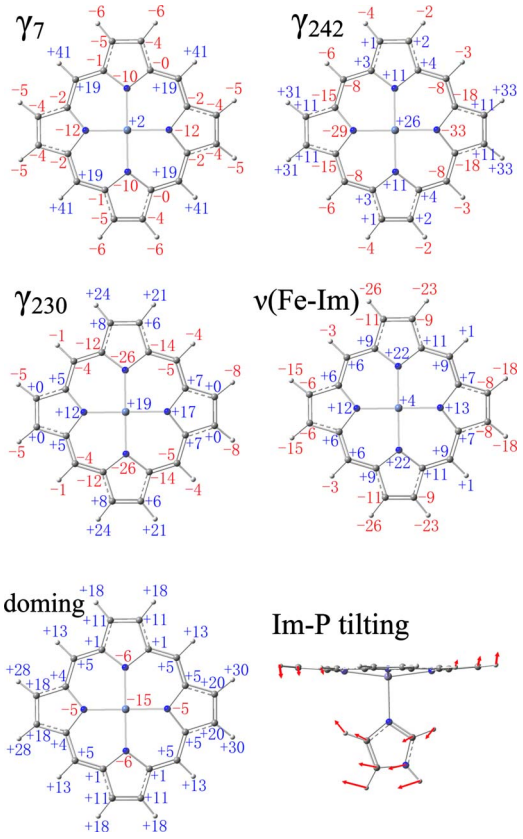

FIG. 6. (Color online) Depiction of the computed five porphine Fe-oop modes and the imidazole-porphine tilting mode. For the five Fe-oop modes, the porphine atom relative displacements are shown by the normalized eigenvectors (scaled by 100) with the directions indicated by the positive or negative signs. The ligand imidazole has the same orientation as in Fig. 1 (not shown here).

Note that all Fe-oop motions identified have significant contribution from the imidazole ligand in their energy transfer pathways. These low frequency modes are presumed to be coupled to the delocalized protein backbone motions in Mb following photodissociation, triggering large-scale protein conformational change, especially in the F helix, toward the deoxyMb equilibrium structure. For example, mode 3, involved in the Fe-oop mode relaxation pathway, was found to be a imidazole-porphine (Im-P) tilting motion (see Fig. 6). It has been suggested that a similar tilting motion plays a central role in the protein structural change in Mb and Hb following ligand binding or dissociation.[50,80,81] The weak coupling and the low frequency characteristic of these modes is the origin of the relatively long time scale related to the protein structure relaxation.[12,28,82,83]

B. Resonant energy transfer between out-of-plane γ_7 and in-plane ν_7 modes

In our simulation, mode 23 (γ_7) was found to be methine wagging motion, with an Fe-oop contribution, in which the Fe motion is correlated with C_m and H_m out-of-plane motions and anticorrelated with pyrrole N motion as demonstrated in Fig. 6. When γ_7 was treated as the system mode, only one important energy transfer pathway was identified due to poor coupling to lower frequency modes, a bad frequency match, or both. On the other hand, analysis of the relaxation of the ν_7 mode, in which it was found that the ν_7 mode couples strongly to the overtone of γ_7, suggests effective energy transfer from the γ_7 Fe-oop motion back to the ν_7 mode. If we assume two quanta excitation of γ_7, which is reasonable for such a low frequency mode following heme excitation,

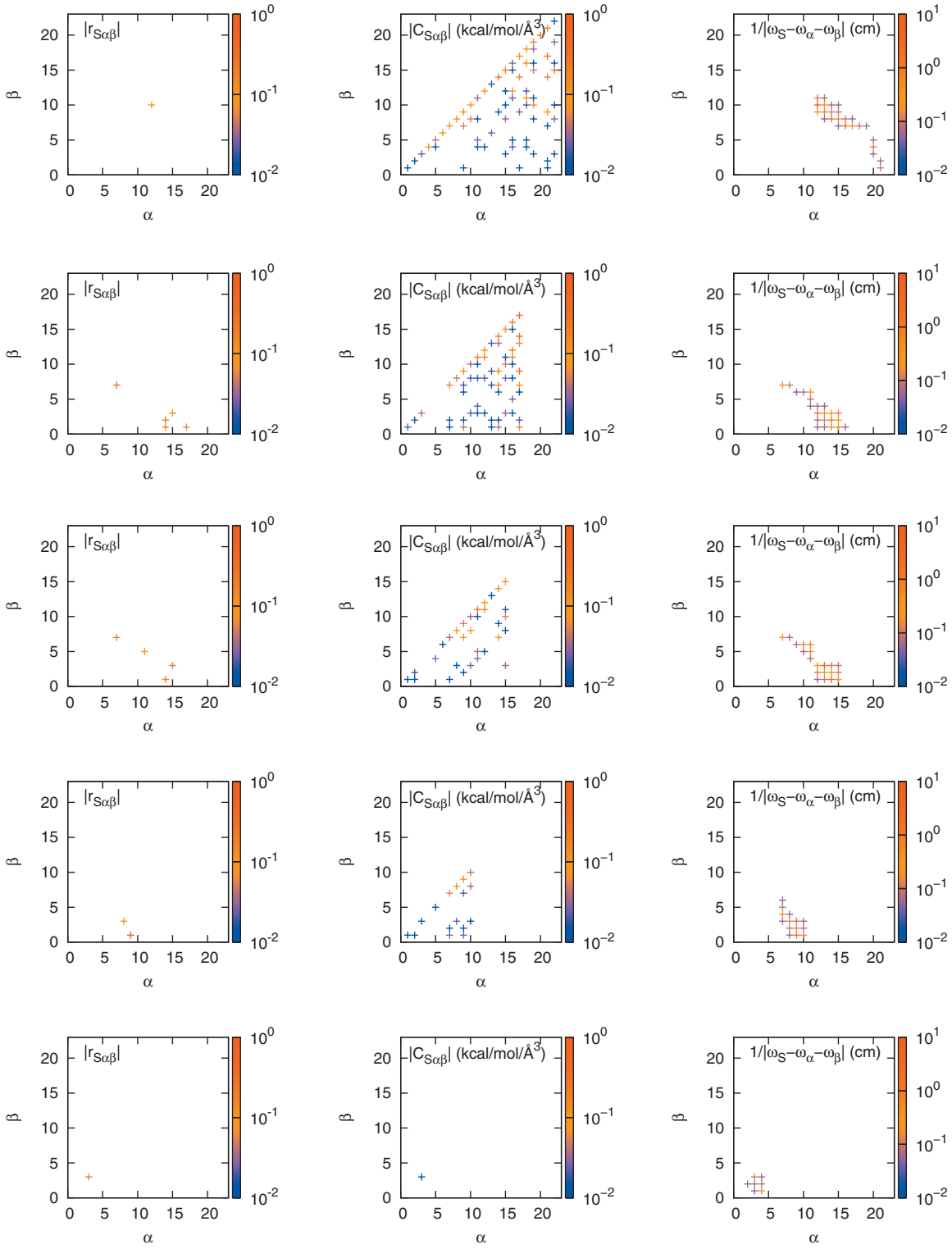

FIG. 7. (Color) The calculated third order Fermi resonance parameter $r_{S\alpha\beta}$ of the important VER pathways for the Fe-oop modes, from top to bottom, γ_7, γ_{242}, γ_{230}, ν(Fe-Im), and the doming motion as well as the important coupling constants $C_{S\alpha\beta}$ and the frequency resonance parameter $1/|\tilde{\omega}_S-\omega_\alpha-\omega_\beta|$. The x and y axes are the indices of the bath modes.

the third order coupling constant for the γ_7 overtone and ν_7 mode was 1.338 kcal/mol Å^3, which is five times larger than any coupling between the γ_7 mode and various low frequency bath modes (see Fig. 7). The Fermi resonance parameter for energy transfer from $\gamma_7+\gamma_7$ to ν_7 was found to be 0.099 (slightly different from ν_7 to $\gamma_7+\gamma_7$ coupling due to the way we deal with the anharmonic correction in the model), larger than any other pathway. The vibrational periods of the γ_7 and ν_7 modes are roughly 100 and 50 fs, respectively, faster than the time resolution of the mode-specific time-resolved resonance Raman spectroscopy experiments (~2 ps).[26–29] The recurring behavior observed in the ν_7 mode density matrix element time profile (see Fig. 4) is caused by this coupling.

C. Enhanced energy transfer in excited electronic state

Our discussion has been based on the properties of electronic ground state of FeP-Im. It has been reported that the heme iron is in the low spin state ($S=0$) in a ligated six-coordinate heme protein, and it changes to an intermediate spin state ($S=1$) in less than 50 fs following diatomic ligand dissociation.[14,42,43,47] This process is accompanied by iron out-of-plane motion and followed by decay to the vibrationally hot electronic ground state ($S=2$) in 300 fs (Ref. 14) with shorter time scale, ~30 fs, also reported.[47] It is not clear which process completes first, the Fe-oop motion or the decay from the electronic excited state to the ground state. It is clear that the Fe-oop motions start before the $S=1$ to $S=2$ transition.[14] This does not complicate the relatively long time scale behavior of VER from the vibrationally excited modes. However, it does affect the initial vibrational excitation process and the relaxation right after that. It is interesting and necessary to check the mode coupling properties in the electronic excited state, especially for those couplings directly related to Fe-oop motion.

Following the same procedure, the VER properties of the ν_4 mode, ν_7 mode, and the Fe-oop motions were calculated for FeP-Im in its excited state ($S=1$). As in the ground state, the Fe-oop motions, with frequencies 358.8 cm^{-1} (mode 21, γ_7), 270.1 cm^{-1} (mode 17), 146.0 cm^{-1} [mode 9, ν(Fe-Im)], and 83.0 cm^{-1} (mode 6, doming), respectively, have significant imidazole motions involved in the dominant energy transfer pathways. In addition, the three lower frequency Fe-oop modes are coupled by overtones. For example, mode 17 couples with the overtone of mode ν(Fe-Im), while mode ν(Fe-Im) couples with the overtone of the doming mode. These couplings make the energy exchange between the Fe-oop modes possible. In addition, the doming mode couples with the overtone of mode 3, which is the Im-P tilting motion with more than 70% of the contribution from the imidazole.

For the FeP-Im in its excited state, mode 21 is the highest frequency Fe-oop mode and is assigned to be the γ_7 mode corresponding to mode 23 in the ground state calculations. The Fe-oop mode 21 is observed to be somewhat decoupled from the other three Fe-oop modes and lower frequency modes. However, its overtone couples with the ν_7 mode even more significantly than in the ground state. The third order coupling constant was found to be 1.565 kcal/mol $Å^3$, which is more than 25 times larger than couplings between mode 21 and its low frequency bath modes. The Fermi resonance parameter for $2\gamma_7$ to ν_7 energy transfer pathway was found to be 0.305, more than six times larger than any other pathway, indicating that this pathway may serve as an efficient channel for the Fe-oop mode relaxation in the excited state.

D. Distinct excitation mechanisms for ν_4 and ν_7 modes

It has been reported that both the ν_4 and ν_7 modes can be highly excited following ligand photodissociation in myoglobin.[26,27,32,34] As demonstrated in Fig. 3, the ν_4 mode is principally porphine Fe–N and N–C stretching motions and can be directly excited through Fe-oop motion. The ν_7 mode is a porphine outer ring breathing-like motion, mainly localized on C_m and H_m atoms, and not structurally coupled to the Fe-oop motions. Based on these observations, it is reasonable to believe that the populations of the ν_4 and ν_7 modes follow distinct excitation mechanisms: the ν_4 mode is directly excited together with the Fe-oop motion, whereas the ν_7 mode is excited by the strongly coupled overtone of the γ_7 Fe-oop motion (mode 21 when $S=1$ or mode 23 when $S=2$). The effect is most pronounced in the electronic excited state. When electronic state changes are involved, such as those associated with ligand photodissociation in heme proteins, the energy transfer mechanism can be overwhelmed by the electronic-vibrational coupling. The electronic-nuclear coupling leads to forces orders of magnitude larger than the vibrational mode-mode coupling that has been the focus of this study, and act on much faster time scales.

The ν_7 mode has been observed to be highly excited following the ligand dissociation in the MbCO coherence spectrum. No similar signal was observed for deoxyMb.[43] Based on femtosecond coherence spectroscopy, Champion and co-workers[38,84] suggested that low frequency vibrational modes associated with electronic rearrangements in the heme iron following ligand photodissociation can be excited simultaneously. We have assumed the separation of the population decay and dephasing processes in our time-dependent perturbation theory. As such, it is beyond the reach of our theory to address the questions concerning mode-mode coherent coupling in these systems.

Due to the poor couplings relative to other Fe-oop modes, indicated by the small third order coupling constants and Fermi resonance parameters, the γ_7 mode was observed to be decoupled from other Fe-oop modes and low frequency modes including those involving imidazole motions. This decoupling may block the energy transfer between the high frequency modes (such as ν_7) and low frequency protein backbone motions through the heme-imidazole connection. This observation provides a possible explanation for the similar heme cooling rates observed in native Mb and the H93G mutant.[45–47]

V. SUMMARY AND CONCLUSIONS

Using a combination of time-dependent perturbation theory[51] and DFT calculations, the mode-specific VER of the imidazole ligated ferrous iron porphine was studied at the UB3LYP/6-31G(d) level. The optimized structure provides a close mimic of the five-coordinate heme moiety in deoxymyoglobin. Seven modes, including ν_4, ν_7, and five modes with iron out-of-plane motion, were independently treated as the system mode with all other heme modes being included explicitly as the bath. The time scale and mechanism for vibrational energy transfer from each system mode were identified with a focus on the interpretation of experimental data on fast energy transfer following heme excitation in myoglobin.

The initial decay process of each system mode was fitted by a single-exponential function. The time constant of 1.7 ± 0.2 ps was derived for the ν_4 mode and ~2.9 ps for the

ν_7 mode. These theoretical predictions, which make no assumptions regarding mechanism, agree well with previous experimental results of Mizutani and Kitagawa[27] for MbCO.

Vibrational energy transfer pathways were identified by calculating the third order Fermi resonance parameters. For the excited ν_4 and ν_7 modes, the important dominant energy transfer pathways involve porphine out-of-plane motions as energy accepting doorway modes. No direct energy transfer between the ν_4 and ν_7 modes was observed.

Cooling of the five Fe-oop modes, including the well-defined heme doming motion and Fe-Im stretching motion, takes place on the picosecond time scale. All modes dissipate vibrational energy through couplings, weaker or stronger, with low frequency out-of-plane modes involving significant imidazole ligand motion. It has been suggested that these couplings trigger the delocalized protein backbone motion, important for protein function, which follows the diatomic ligand dissociation in Mb. With the exception of the highest frequency γ_7 mode, these Fe-oop modes couple to one another through overtones in the electronic excited state.

The γ_7 mode, a porphine methine wagging motion associated with Fe-oop motion, is believed to be directly excited following ligand photodissociation in MbCO. The coupling of this mode to lower frequency bath modes is predicted to be very weak. However, its overtone is strongly coupled to the ν_7 mode, forming an effective energy transfer pathway for relaxation on the electronic ground state and excited state surfaces. This strong coupling suggests a possible mechanism of excitation of the ν_7 mode through energy transfer from the γ_7 mode. That mechanism is distinctly different than direct excitation together with Fe-oop motion of the ν_4 mode and provides support for earlier conjectures of directed mode-specific energy transfer following ligand dissociation in myoglobin.

ACKNOWLEDGMENTS

We are grateful for the generous support of this research by the National Science Foundation (Nos. CHE-0316551 and CHE-0750309) and Boston University's Center for Computer Science. We thank Professor Paul M. Champion for useful discussions and many helpful comments.

[1] M. C. Asplund, M. T. Zanni, and R. M. Hochstrasser, Proc. Natl. Acad. Sci. U.S.A. **97**, 8219 (2000).
[2] Y. Kholodenko, M. Volk, E. Gooding, and R. M. Hochstrasser, Chem. Phys. **259**, 71 (2000).
[3] E. Münck and P. M. Champion, Ann. N.Y. Acad. Sci. **244**, 142 (1975).
[4] J. T. Sage, C. Paxson, G. R. A. Wyllie, W. Sturhahn, S. M. Durbin, P. M. Champion, E. E. Alp, and W. R. Scheidt, J. Phys.: Condens. Matter **13**, 7707 (2001).
[5] J. T. Sage, S. M. Durbin, W. Sturhahn, D. C. Wharton, P. M. Champion, P. Hession, J. Sutter, and E. E. Alp, Phys. Rev. Lett. **86**, 4966 (2001).
[6] E. R. Henry, W. A. Eaton, and R. M. Hochstrasser, Proc. Natl. Acad. Sci. U.S.A. **83**, 8982 (1986).
[7] E. R. Henry and R. M. Hochstrasser, Proc. Natl. Acad. Sci. U.S.A. **84**, 6142 (1987).
[8] R. Elber and M. Karplus, Science **235**, 318 (1987).
[9] R. Elber and M. Karplus, J. Am. Chem. Soc. **112**, 9161 (1990).
[10] R. J. D. Miller, Annu. Rev. Phys. Chem. **42**, 581 (1991).
[11] J. E. Straub and M. Karplus, Chem. Phys. **158**, 221 (1991).
[12] H. Li, R. Elber, and J. E. Straub, J. Biol. Chem. **268**, 17908 (1993).
[13] I. Okazaki, Y. Hara, and M. Nagaoka, Chem. Phys. Lett. **337**, 151 (2001).
[14] J. W. Petrich, C. Poyart, and J. L. Martin, Biochemistry **27**, 4049 (1988).
[15] T. Lian, B. Locke, Y. Kholodenko, and R. M. Hochstrasser, J. Phys. Chem. **98**, 11648 (1994).
[16] Y. Zhang, H. Fujisaki, and J. E. Straub, J. Phys. Chem. B **111**, 3243 (2007).
[17] M. Walther, V. Raicu, J. P. Ogilvie, R. Phillips, R. Kluger, and R. J. D. Miller, J. Phys. Chem. B **109**, 20605 (2005).
[18] A. M. Nagy, V. Raicu, and R. J. D. Miller, Biochim. Biophys. Acta **1749**, 148 (2005).
[19] J. R. Hill, A. Tokmakoff, K. A. Peterson, B. Sauter, D. Zimdars, D. D. Dlott, and M. D. Fayer, J. Phys. Chem. **98**, 11213 (1994).
[20] K. D. Rector, C. W. Rella, J. R. Hill, and A. S. Kwok, S. G. Sligar, E. Y. P. Chien, D. D. Dlott, and M. D. Fayer, J. Phys. Chem. B **101**, 1468 (1997).
[21] K. D. Rector, J. Jiang, M. A. Berg, and M. D. Fayer, J. Phys. Chem. B **105**, 1081 (2001).
[22] I. J. Finkelstein, A. Goj, B. McClain, A. M. Massari, K. A. Merchant, R. F. Loring, and M. D. Fayer, J. Phys. Chem. B **109**, 16959 (2005).
[23] A. Xie, W. van Der Meer, L. Hoff, and R. H. Austin, Phys. Rev. Lett. **84**, 5435 (2000).
[24] H. Frauenfelder and B. H. McMahon, BioSystems **62**, 3 (2001).
[25] R. Elber and Q. H. Gibson, J. Phys. Chem. B **112**, 6147 (2008).
[26] Y. Mizutani and T. Kitagawa, Science **278**, 443 (1997).
[27] Y. Mizutani and T. Kitagawa, Chem. Rec. **1**, 258 (2001).
[28] S. G. Kruglik, P. Mojzes, Y. Mizutani, T. Kitagawa, and P.-Y. Turpin, J. Phys. Chem. B **105**, 5018 (2001).
[29] T. Kitagawa, N. Haruta, and Y. Mizutani, Biopolymers **61**, 207 (2002).
[30] J. Rodriguez and D. Holten, J. Chem. Phys. **91**, 3525 (1989).
[31] J. Rodriguez, C. Kirmaier, and D. Holten, J. Chem. Phys. **94**, 6020 (1991).
[32] Y. Mizutani and T. Kitagawa, Bull. Chem. Soc. Jpn. **75**, 623 (2002).
[33] Y. Mizutani, Y. Uesugi, and T. Kitagawa, J. Chem. Phys. **111**, 8950 (1999).
[34] Y. Mizutani and T. Kitagawa, J. Mol. Liq. **90**, 233 (2001).
[35] Y. Mizutani and T. Kitagawa, Bull. Chem. Soc. Jpn. **75**, 965 (2002).
[36] F. Rosca, A. T. N. Kumar, X. Ye, T. Sjodin, A. A. Demidov, and P. M. Champion, J. Phys. Chem. A **104**, 4280 (2000).
[37] F. Rosca, A. T. N. Kumar, D. Ionascu, T. Sjodin, A. A. Demidov, and P. M. Champion, J. Chem. Phys. **114**, 10884 (2001).
[38] F. Rosca, A. T. N. Kumar, D. Ionascu, X. Ye, A. A. Demidov, T. Sjodin, D. Wharton, D. Barrick, S. G. Sligar, T. Yonetani, and P. M. Champion, J. Phys. Chem. A **106**, 3540 (2002).
[39] P. M. Champion, F. Rosca, D. Ionascu, W. Cao, and X. Ye, Faraday Discuss. **127**, 123 (2004).
[40] F. Gruia, X. Ye, D. Ionascu, M. Kubo, and P. M. Champion, Biophys. J. **93**, 4404 (2007).
[41] F. Gruia, M. Kubo, X. Ye, D. Lonascu, C. Lu, R. K. Poole, S.-R. Yeh, and P. M. Champion, J. Am. Chem. Soc. **130**, 5231 (2008).
[42] W. Wang, A. A. Demidov, X. Ye, J. F. Christian, T. Sjodin, and P. M. Champion, J. Raman Spectrosc. **31**, 99 (2000).
[43] M. R. Armstrong, J. P. Ogilvie, M. L. Cowan, A. M. Nagy, and R. J. D. Miller, Proc. Natl. Acad. Sci. U.S.A. **100**, 4990 (2003).
[44] M. Lim, T. A. Jackson, and P. A. Anfinrud, J. Phys. Chem. **100**, 12043 (1996).
[45] D. E. Sagnella and J. E. Straub, J. Phys. Chem. B **105**, 7057 (2001).
[46] L. Bu and J. E. Straub, J. Phys. Chem. B **107**, 10634 (2003).
[47] X. Ye, A. Demidov, F. Rosca, W. Wang, A. Kumar, D. Ionascu, L. Zhu, D. Barrick, D. Wharton, and P. M. Champion, J. Phys. Chem. A **107**, 8156 (2003).
[48] Y. Gao, M. Koyama, S. F. El-Mashtoly, T. Hayashi, K. Harada, Y. Mizutani, and T. Kitagawa, Chem. Phys. Lett. **429**, 239 (2006).
[49] M. Koyama, S. Neya, and Y. Mizutani, Chem. Phys. Lett. **430**, 404 (2006).
[50] G. S. Kachalova, A. N. Popov, and H. D. Bartunik, Science **284**, 473 (1999).
[51] H. Fujisaki, Y. Zhang, and J. E. Straub, J. Chem. Phys. **124**, 144910 (2006).
[52] H. Fujisaki and J. E. Straub, J. Phys. Chem. B **111**, 12017 (2007).
[53] G. B. Jameson, F. S. Molinaro, J. A. Ibers, J. P. Collman, J. I. Brauman, E. Rose, and K. S. Suslick, J. Am. Chem. Soc. **102**, 3224 (1980).
[54] W. R. Scheidt and C. Reed, Chem. Rev. (Washington, D.C.) **81**, 543 (1981).
[55] C. Hu, A. Roth, M. K. Ellison, J. An, C. M. Ellis, C. E. Schulz, and W. R. Scheidt, J. Am. Chem. Soc. **127**, 5675 (2005).

[56] C. Hu, J. An, B. C. Noll, C. E. Schulz, and W. R. Scheidt, Inorg. Chem. **45**, 4177 (2006).
[57] H. Fujisaki, L. Bu, and J. E. Straub, Adv. Chem. Phys. **130**B, 179 (2005).
[58] M. J. Frisch, G. W. Trucks, H. B. Schlegel *et al.*, GAUSSIAN 03, Revision C.02, Gaussian, Inc., Wallingford, CT, 2004.
[59] M. E. Cremeens, H. Fujisaki, Y. Zhang, J. Zimmermann, L. B. Sagle, S. Matsuda, P. E. Dawson, J. E. Straub, and F. E. Romesberg, J. Am. Chem. Soc. **128**, 6028 (2006).
[60] H. Fujisaki, K. Yagi, K. Hirao, and J. E. Straub, Chem. Phys. Lett. **443**, 6 (2007).
[61] K. Moritsugu, O. Miyashita, and A. Kidera, J. Phys. Chem. B **107**, 3309 (2003).
[62] C. Rovira, K. Kune, J. Hutter, P. Ballone, and M. Parrinello, J. Phys. Chem. A **101**, 8914 (1997).
[63] P. M. Kozlowski, T. G. Sprio, and M. Z. Zgierski, J. Phys. Chem. B **104**, 10659 (2000).
[64] D. A. Scherlis and D. A. Estrin, Int. J. Quantum Chem. **87**, 158 (2002).
[65] D. Scherlis, M. Cococcioni, P. Sit, and N. Marzari, J. Phys. Chem. B **111**, 7384 (2007).
[66] J. L. Hoard, *Stereochemistry of Porphyrins and Metalloporphyrins* (Elsevier Scientific, New York, 1975), Chap. 8, p. 356.
[67] J. Kuriyan, S. Wilz, M. Karplus, and G. A. Petsko, J. Mol. Biol. **192**, 133 (1986).
[68] L. Schlichting, J. Berendzen, J. Phillips, N. George, and R. M. Sweet, Nature (London) **371**, 808 (1994).
[69] See EPAPS Document No. E-JCPSA6-130-004903 for supplementary material. For more information on EPAPS, see http://www.aip.org/pubservs/epaps.html.
[70] J. Deak, H.-L. Chiu, C. M. Lewis, and R. J. D. Miller, J. Phys. Chem. B **102**, 6621 (1998).
[71] V. Srajer, R. Reinisch, and P. M. Champion, J. Am. Chem. Soc. **110**, 6656 (1988).
[72] X. Ye, D. Lonascu, F. Gruia, A. Yu, A. Benabbas, and P. M. Champion, Proc. Natl. Acad. Sci. U.S.A. **104**, 14682 (2007).
[73] D. D. Klug, M. Z. Zgierski, J. S. Tse, Z. Liu, J. R. Kincaid, and K. Czarneck, Proc. Natl. Acad. Sci. U.S.A. **99**, 12526 (2002).
[74] S. Franzen, C. Poyart, and J. L. Martin, Biochemistry **34**, 1224 (1995).
[75] K. R. Rodgers and T. G. Spiro, Science **265**, 1697 (1994).
[76] A. Sato and Y. Mizutani, Biochemistry **44**, 14709 (2005).
[77] A. Sato, Y. Gao, T. Kitagawa, and Y. Mizutani, Proc. Natl. Acad. Sci. U.S.A. **104**, 9627 (2007).
[78] P. M. Kozlowski, T. G. Sprio, A. Berces, and M. Z. Zgierski, J. Phys. Chem. B **102**, 2603 (1998).
[79] T. G. Spiro, P. M. Kozlowski, and M. Z. Zgierski, J. Raman Spectrosc. **29**, 869 (1998).
[80] B. R. Gelin and M. Karplus, Proc. Natl. Acad. Sci. U.S.A. **74**, 801 (1977).
[81] J. M. Friedman, T. W. Scott, and R. A. Stepnoski, J. Biol. Chem. **258**, 10564 (1983).
[82] E. W. Findsen, T. W. Scott, M. R. Chance, J. M. Friedman, and M. R. Ondrias, J. Am. Chem. Soc. **107**, 3355 (1985).
[83] X. Xie and J. D. Simon, Biochemistry **30**, 3682 (1991).
[84] L. Zhu, T. Sage, and P. M. Champion, Science **266**, 629 (1994).